AIAA JOURNAL
Vol. 43, No. 12, December 2005

Technical Notes

TECHNICAL NOTES are short manuscripts describing new developments or important results of a preliminary nature. These Notes should not exceed 2500 words (where a figure or table counts as 200 words). Following informal review by the Editors, they may be published within a few months of the date of receipt. Style requirements are the same as for regular contributions (see inside back cover).

Laser Doppler Measurements of a Highly Curved Flow

J. M. M. Barata*
Universidade da Beira Interior, 6201-001 Covilhã, Portugal
and
D. F. G. Durão†
Universidade Lusíada, 1349-001 Lisbon, Portugal

Nomenclature

U = horizontal velocity, $\bar{U} + u'$
V = vertical velocity, $\bar{V} + v'$
X = horizontal coordinate (positive in the direction of the boundary layer)
Y = vertical coordinate (positive upward)

Subscripts

j = wall jet
0 = boundary layer

Introduction

HIGHLY curved flows are quite common in nature and frequently originate by impermeable surfaces that deflect a flow. This type of complex flow is characterized by complicating influences, such as extra rates of strain and enhanced turbulence production through the interaction of normal stresses with normal strains.[1,2] In addition, it is typical of impingement cooling applications in industry, as well as of the flow beneath a short/vertical takeoff aircraft that is lifting off or landing with zero or small forward momentum. In this latter application, the impingement of the lift jets on the ground results in the formation of a wall jet that flows radially from the impinging point along the ground surface[3] that interacts strongly with the ground plane resulting in lift losses, in enhanced entrainment close to the ground (suckdown), in engine thrust losses following reingestion of the exhaust gases, and in possible aerodynamic instabilities caused by fountain impingement on the aircraft underside. The interaction of this wall jet with the freestream results in the formation of a highly curved flow (ground or scarf vortex) far upstream of the impinging jet that has profound influences on the flow development.

Measurements of this type of flow are very scarce and have only been reported in the context of a secondary flow within the impinging jet flow problem.[4–6] Recently, Barata and Durão[1] found that the shape, size, and location of the ground vortex were dependent on the ratio between the jet exit and the crossflow velocities, and two different regimes were identified. One is characterized by the contact between the ground vortex and the impinging jet, whereas another is detached upstream of the impinging zone. They also report that the crossflow acceleration over the ground vortex was directly connected with the jet exit velocity and the influence of the upstream wall jet was not confined to the ground vortex but spread upward by a mechanism not very well known yet.

This Note presents a study of the highly curved flow resulting from the impingement of a wall jet with a boundary layer and aims to improve the understanding of the ground vortex behavior. The influence of the impinging region on the curved flow region is eliminated by producing independently a wall jet using a two-dimensional configuration similar to the upwash flow of Gilbert.[7] The wall jet impinges with the boundary layer produced using a conventional wind tunnel, giving rise to a highly curved flow, which can be studied for different velocity ratios between the wall jet and crossflow (Fig. 1).

Experimental Method and Procedures

The wind-tunnel facility designed and constructed for the present study is diagramed in Fig. 1. The recommendations of Metha and Bradshaw[8] for open-circuit wind tunnels were followed throughout the design process, especially for the boundary-layer part of the flow. A fan of 15-kW nominal power drives a maximum flow of 3000 m^3/h through the boundary layer and the wall jet tunnels of 300×400 mm and 40×400 mm exit sections, respectively. The facility was built to allow variable heights of the wall jet exit, but in the present study, a single value of 40 mm was used.

The origin of the horizontal X and vertical Y coordinates is taken near the visual maximum penetration point in the ground plane at 750 mm downstream of the boundary-layer wind-tunnel exit. The X coordinate is positive in the boundary-layer direction, and Y is positive upward.

The present results were obtained in the vertical plane of symmetry (spanwise midplane) for a wall jet mean velocity of $U_j = 6$ m/s and a mean boundary-layer velocity of $U_0 = 3.48$ m/s, corresponding to a velocity ratio of 1.7.

The velocity field was measured with a laser Doppler velocimeter, which comprised a 10-mW He–Ne and a 25-mW Nd:YAG laser, with sensitivity to the flow direction provided by frequency shifting from a Bragg cell at $f_0 = 40$ MHz and a transmission and backward-scattered light collection focal lens of 400 mm. The half-angle between the beams was 2.8 and the calculated dimensions of the axis of the measuring ellipsoid volume at the e^{-2} intensity locations were $135 \times 6.54 \times 6.53$ μm and $112 \times 5.46 \times 5.45$ μm, respectively. The horizontal U and vertical V mean and turbulent velocities together with the shear stress $\overline{u'v'}$ were determined by a two channel Dantec BSA F60 processor. The principal characteristics of the laser Doppler velocimeter (LDV) are summarized in Table 1. The seeding of the flow with glycerine particles of 0.1–5 μm was produced with medical atomizers operating at 1.5 bar. The transmitting and collecting optics are mounted on a three-dimensional transversing unit, allowing the positioning of the probe volume within ± 0.1 mm.

The largest statistical errors derived from populations of 10,000 velocity values were 0.5 and 3%, respectively, for the mean and variance values for a 95% confidence interval. For each burst, the arrival time and the transit time of the seeding particle were recorded.

Presented as Paper 2005-0064 at the 43rd Aerospace Sciences Meeting, Reno, NV, 10–13 January 2005; received 27 January 2005; revision received 17 June 2005; accepted for publication 18 July 2005.

*Full Professor, Aerospace Sciences Department. Associate Fellow AIAA.
†Full Professor.

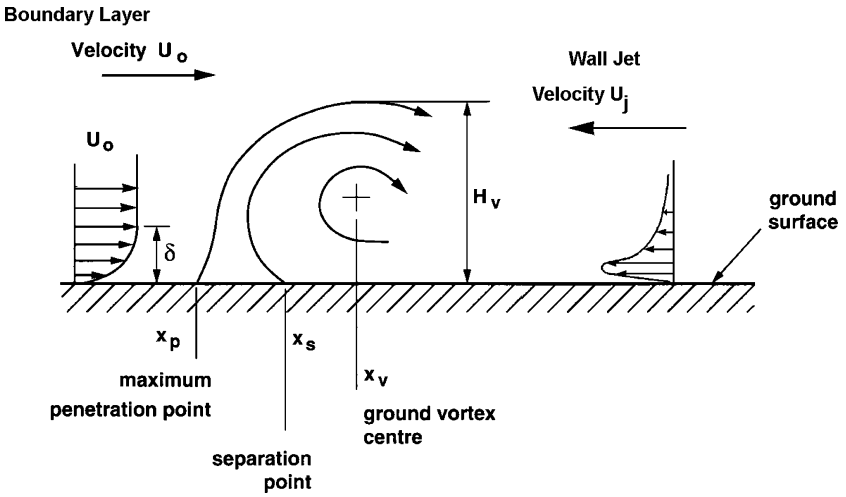

Fig. 1 Ground vortex facility.

Table 1 Principal characteristics of the laser Doppler velocimeter

Property	Red	Green
Wavelength λ, nm	633	532
Focal length of focusing lens f, mm	400	400
Beam diameter at e^{-2} intensity, mm	1.35	1.35
Beam spacing s, mm	38.87	39.13
Calculated half-angle of beam intersection θ, deg	2.78	2.8
Fringe spacing δ_f, μm	6.53	5.45
Velocimeter transfer constant K, MHz/ms^{-1}	0.153	0.183

No corrections were made for sampling bias, but no correlations were found between Doppler frequencies and time interval between consecutive bursts, suggesting that those effects are unimportant for the present flow conditions. The calculation of the two components of the mean and rms velocities, and the Reynolds shear stress were performed for coincident velocity samples.

Results and Discussion

Experimental visualization studies were performed using direct digital photography and a smoke generator to produce the tracer particles. The visualization results of the present complex flow were used to provide a first insight into the nature of the flow and to guide the choice of quantitative measurement locations. The wall jet impinges on the boundary layer and is strongly deflected backward at an average angle of 36 deg with the ground surface (Fig 2).

Figure 3 shows the mean velocity obtained from the LDV measurements of the mean horizontal $\bar{U}$ and vertical $\bar{V}$ velocity components, which confirm the preceding description of the flow and quantify the mean flow characteristics of the impingement zone. Based on the stream trace lines, it is expected that the maximum penetration point occurs at $X = 85$ mm and that the centerline of the deflected flow has an inclination angle with the ground plane of 40 deg. The inclination of the deflected wall jet is also clearly noticed from the zero values of the mean velocity (dashed line, Fig. 3), which corresponds to an inclination angle of 32 deg. In the impingement zone, both wall jet and boundary-layer fluid move toward the wall, giving rise to an extremely complex flow, which includes a small secondary vortex flow on the boundary-layer side near the ground plane ($Y < 20$ mm and $40 < X < 85$ mm) that seems to entrain fluid from the lower part of the wall jet.

The analysis of the flow can be further documented with the help of Figs. 4 and 5, which show horizontal profiles of $\sqrt{u'^2}$ and $\sqrt{v'^2}$ and quantify the turbulence characteristics of the impingement zone and deflected wall jet flow. The profiles show intense velocity fluctuations with peaks that are difficult to identify clearly or to relate with mean velocity gradients. The measured velocity probability distributions are nearly Gaussian, suggesting the absence of discrete frequency oscillations, but no power spectra analysis was performed.

Fig. 2 Visualization of the flow, $U_j = 6$ m/s and $U_0 = 3.48$ m/s.

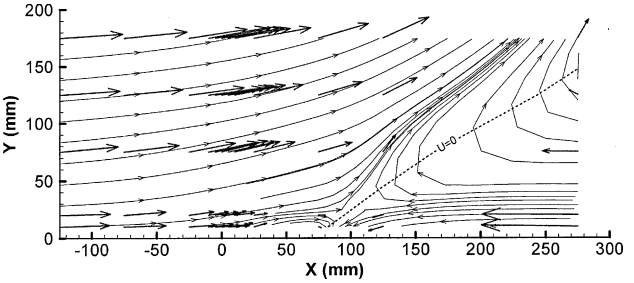

Fig. 3 Mean velocity field obtained from the LDV measurements and stream trace lines.

The flow is anisotropic in that, with the exception of the inclined upwash flow region, $\sqrt{u'^2}$ is largest in the boundary layer, wall jet, and impingement zone. The peaks of $\sqrt{u'^2}$ are larger than the corresponding peaks of $\sqrt{v'^2}$ in the impingement zone, giving rise to high levels of anisotropy, with $\sqrt{u'^2}/\sqrt{v'^2} \approx 3$, whereas in the deflected upwash flow region the vertical normal stress is the largest and the corresponding level of anisotropy is $\sqrt{u'^2}/\sqrt{v'^2} \approx 0.7$.

The distribution of the shear stress $\overline{u'v'}$ may be analyzed on the basis of Fig. 6. The impingement zone (near the ground plane) is dominated by the mean shear strains $\partial\bar{V}/\partial Y$, $\partial\bar{U}/\partial X$, and $\partial\bar{U}/\partial Y$, whereas in the upwash deflected flow region $\partial\bar{V}/\partial X$, and $\partial\bar{U}/\partial Y$ assume the largest values. Additionally, note that $\partial\bar{U}/\partial Y$ is uniformly larger than $\partial\bar{U}/\partial X$ (about 1.38 times) for the region of study. Thus, in the upwash deflected region, the sign of the shear stress is related to that of the shear strain in accordance with a turbulent viscosity hypothesis. In the impingement zone, the two shear strains and the normal strain $\partial\bar{U}/\partial X$ have the same order of magnitude, and the thin shear-layer approximation, as already reported by Barata et al.,[9] Bradshaw,[10] and Castro and Bradshaw,[11] is not valid. When the profile of $\overline{u'v'}$ at $Y = 10$ mm is analyzed, the regions where the shear layer approximation is invalid are located in the boundary layer when it starts to be deflected upward due to the influence of

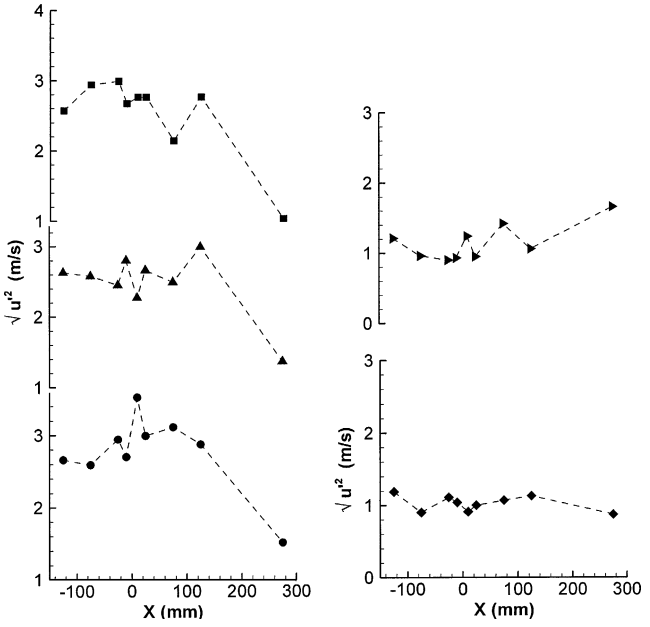

Fig. 4 Horizontal profiles of fluctuating horizontal velocity component $\sqrt{u'^2}$: ●, $Y = 10$ mm; ▲, $Y = 20$ mm; ■, $Y = 75$ mm; ♦, $Y = 125$ mm; and ►, $Y = 175$ mm.

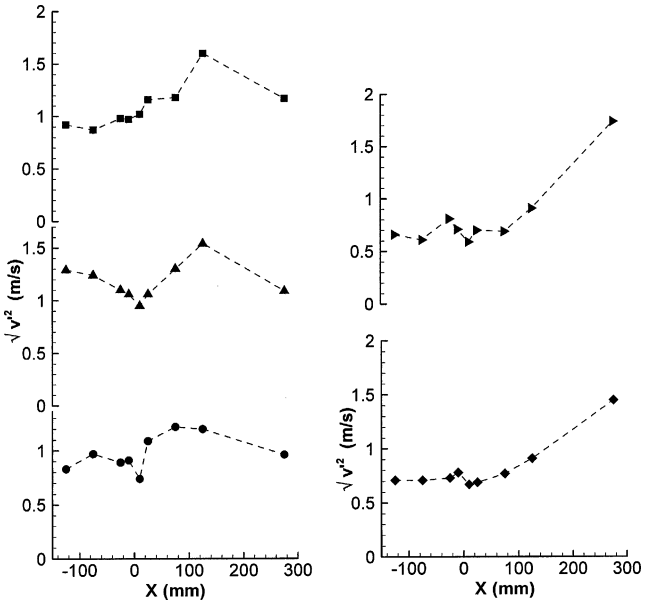

Fig. 5 Horizontal profiles of fluctuating vertical velocity component $\sqrt{v'^2}$: ●, $Y = 10$ mm; ▲, $Y = 20$ mm; ■, $Y = 75$ mm; ♦, $Y = 125$ mm; and ►, $Y = 175$ mm.

the small ground vortex ($-20 < X < 5$ mm) and near the stagnation point ($90 < X < 120$ mm). The Reynolds stress decrease in the regions of high stabilizing curvature typical of the impinging zones can also be confirmed by the profiles obtained at $Y = 20$ mm and $Y = 75$ mm.

The present results show that the turbulence structure of a highly curved flow is subject to the flow distortion and is influenced by the competing magnitudes of mean normal and shear strains $\partial\bar{U}/\partial X$, $\partial\bar{U}/\partial Y$, and $\partial\bar{V}/\partial Y$. Consequently, the engineering calculation methods that usually adopt principles for well-behaved shear layers, such as the estimation of a length scale from the thin shear-layer thickness or the gradient diffusion hypothesis for turbulent transport, need to be applied with caution, and a careful analysis of the predicted turbulent flowfield should always be performed.

Figure 3 has shown the upward deflected flow due to the impingement of the wall jet and the boundary layer, and has revealed the

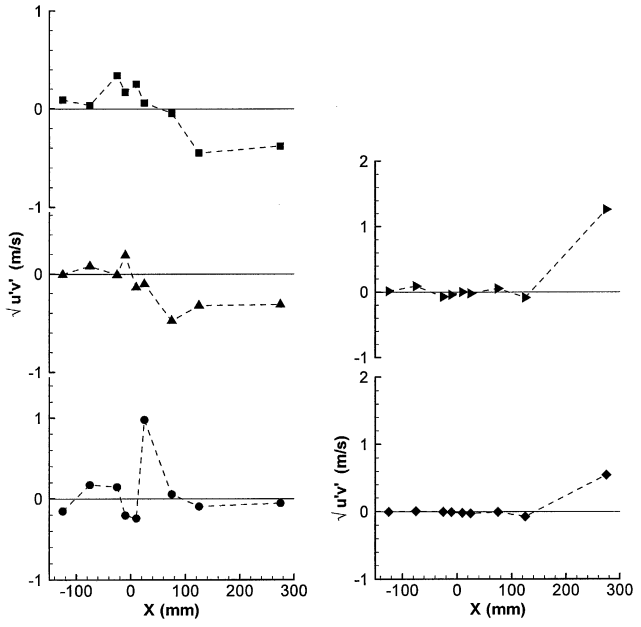

Fig. 6 Horizontal profiles of Reynolds shear stress $\overline{u'v'}$: ●, $Y = 10$ mm; ▲, $Y = 20$ mm; ■, $Y = 75$ mm; ♦, $Y = 125$ mm; and ►, $Y = 175$ mm.

small secondary vortex flow on the boundary-layer side near the ground plane, $Y < 20$ mm and $40 < Y < 85$ mm. Barata and Durão[1] reported two different influences for the ground vortex development: one related to the impingement of the wall jet and the crossflow and another mainly associated with the enhanced flow entrainment produced by the high-velocity impinging jet. The present study provides additional information for the impingement zone corresponding to the first factor (region 1) but should not be used to extrapolate any influence of the impinging jet (region 2).

Conclusions

Laser Doppler measurements of velocity characteristics of the flowfield resulting from the impingement of a wall jet with a boundary layer are presented and discussed together with visualization of the flow. The experiments have been carried out for wall jet and boundary-layer velocities of 6 and 3.48 m/s, respectively.

The present study provides additional information for the impingement zone of the ground vortex development reported by Barata and Durão.[1] The results show that the wall jet impinges with the boundary layer and is strongly deflected backward with an average angle of 36 deg with the ground surface. In the impingement zone, both wall jet and boundary layer fluid move toward the wall, giving rise to an extremely complex flow, which includes a small secondary vortex flow on the boundary-layer side near the ground plane that seems to entrain fluid from the lower part of the wall jet.

The present flow is characterized by intense velocity fluctuations with peaks that are difficult to identify clearly or to relate with mean velocity gradients. The measured velocity probability distributions are nearly Gaussian, suggesting the absence of discrete frequency oscillations, but no power spectra analysis was performed.

In common with other complex turbulent flows, the turbulence is anisotropic with the relative magnitude of normal and shear stresses changing along the flow. In the upwash deflected region, the sign of the shear stress is consistent with the sign of the shear strain in accordance with a turbulent viscosity hypothesis. However, in the region where the boundary layer starts to be deflected upward due to the influence of the small ground vortex, and near the stagnation point, large effects of flow distortion on the turbulence structure are expected.

Acknowledgments

The present work was performed within the scope of activities of the Center for Aerospace Sciences and Technologies, funded by

Fundação para a Ciência e Tecnologia (Research Unit 151) within the scope of the European POCTI Program.

References

[1]Barata, J. M. M., and Durão, D. F. G., "Laser-Doppler Measurements of Impinging Jets Through a Crossflow," *Experiments in Fluids*, Vol. 36, No. 5, 2004, pp. 117–129.

[2]Castro, I. P., and Bradshaw, P., "The Turbulence Structure of a Highly Curved Mixing Layer," *Journal of Fluid Mechanics*, Vol. 73, Pt. 2, 1976, pp. 265–304.

[3]Barata, J. M. M., "Experimental and Numerical Study on the Aerodynamics of Impinging Jets in a Crossflow," Ph.D. Dissertation, Mechanical Engineering Dept., Inst. Superior Técnico, Technical Univ., Lisbon, 1989 (in Portuguese).

[4]Barata, J. M. M., Durão, D. F. G., Heitor, M. V., and McGuirk, J. J., "On the Analysis of an Impinging Jet on Ground Effects," *Experiments in Fluids*, No. 15, 1993, pp. 117–129.

[5]Barata, J. M. M., "Fountain Flows Produced by Multiple Impinging Jets in a Crossflow," *AIAA Journal*, Vol. 34, No. 12, 1996, pp. 2523–2530.

[6]Knowles, K., and Bray, D., "The Ground Vortex Formed by Impinging Jets in Crossflow," AIAA Paper 91-0768, Jan. 1991.

[7]Gilbert, B. L., "Detailed Turbulence Measurements in a Two-Dimensional Upwash," AIAA Paper 83-1678, July 1983.

[8]Metha, R. D., and Bradshaw, P., "Design Rules for Small Low-Speed Wind Tunnels," *Aeronautical Journal*, Nov. 1979, pp. 443–449.

[9]Barata, J. M. M., Durão, D. F. G., and McGuirk, J. J., "Numerical Study of Single Impinging Jets Through a Crossflow," *Journal of Aircraft*, Vol. 26, No. 11, 1989, pp. 1002–1008.

[10]Bradshaw, P., "Effects of Streamline Curvature on Turbulent Flow," AGARDograph, Vol. 169, 1973.

[11]Castro, I. P., and Bradshaw, P., "The Turbulence Structure of a Highly Curved Mixing Layer," *Journal of Fluid Mechanics*, Vol. 73, 1976, pp. 265–304.

R. Lucht
Associate Editor